Proceedings of the ASME 2021 Heat Transfer Summer Conference
HT2021
June 16-18, 2021, Virtual, Online

HT2021-62417

Comparison of Radiation Models for a Turbulent Piloted Methane/Air Jet Flame: A Frozen-Field Study

Chloe David
Opus College of Engineering
Marquette University
Milwaukee, WI 53233
Email: chloe.david@marquette.edu

Wenjun Ge *
Computational Sciences and
Engineering Division
Oak Ridge National Laboratory
Oak Ridge, TN 37831
Email: gew1@ornl.gov

Somesh P. Roy
Opus College of Engineering
Marquette University
Milwaukee, WI 53233
Email: somesh.roy@marquette.edu

Michael F. Modest
School of Engineering
University of California, Merced
Merced, CA 95343
Email: mmodest@ucmerced.edu

Ramanan Sankaran
Computational Sciences and
Engineering Division
Oak Ridge National Laboratory
Oak Ridge, TN 37831
Email: sankaranr@ornl.gov

ABSTRACT

Numerical modeling of radiative transfer in nongray reacting media is a challenging problem in computational science and engineering. The choice of radiation models is important for accurate and efficient high-fidelity combustion simulations. Different applications usually involve different degrees of complexity, so there is yet no consensus in the community. In this paper, the performance of different radiative transfer equation (RTE) solvers and spectral models for a turbulent piloted methane/air jet flame are studied. The flame is scaled from the Sandia Flame D with a Reynolds number of 22,400. Three classes of RTE solvers, namely the discrete ordinates method, spherical harmonics method, and Monte Carlo method, are examined. The spectral models include the Planck-mean model, the full-spectrum k-distribution (FSK) method, and the line-by-line (LBL) calculation. The performances of different radiation models in terms of accuracy and computational cost are benchmarked. The results have shown that both RTE solvers and spectral models are critical in the prediction of radiative heat source terms for this jet flame. The trade-offs between the accuracy, the computational cost, and the implementation difficulty are discussed in detail. The results can be used as a reference for radiation model selection in combustor simulations.

INTRODUCTION

Modeling of radiative transfer is important for high-fidelity combustion simulations, flame diagnostics, and combustor designs. Significant progresses have been achieved in the past decades in both spectral models and numerical solvers for the radiative transfer equation (RTE) [1]. However, the choice of radiation models is still an open question due to different degrees of complexity in combustion problems. The selection of radi-

*Address all correspondence to this author.

ation models is difficult for both theoretical and practical reasons. One reason is the strongly varying spectral property of the gases. The major gaseous products (CO_2, H_2O and CO) from the combustion of hydrocarbons have millions of broadened spectral lines. Although the spectral knowledge is now available through the high-resolution spectroscopic databases [2–4], a line-by-line (LBL) calculation is still impractical for most deterministic solution methods except for Monte Carlo-based solvers with sufficient sampling points. Therefore, efficient spectral models are required to keep the computational cost within a reasonable range. Another difficulty is that both the accuracy and speed of the RTE solvers are case-dependent. Combustion involves emitting and absorbing gases with strong spectral dependency, so there is no simple way to characterize the radiative transfer and to pick the proper RTE solver accordingly. One dimensionless number that is often used to characterize a radiation problem is the optical thickness. When the optical thickness is large, the radiative intensity tends to be more isotropic. For an optically intermediate case, the radiative intensity is expected to be more anisotropic. For an optically thin case, one can even safely skip the solution of the RTE directly, which is called the Optically Thin model. One should be able to identify the optimal RTE solver based on the optical thickness for relatively simple problems. However, the concept of optical thickness is a rough estimation, which is not defined well for nongray problems and multidimensional nonhomogeneous media as found in most flame simulations.

The RTE is an integro-differential equation in five dimensions (three in space, and two in direction). The angular dependency of the RTE makes it exceedingly difficult to solve for realistic radiative transfer problems. Except for very simple cases where analytical solutions are available, the solution method needs to approximate the angular distributions of the radiative intensity. A detailed description of different RTE solvers and spectral models can be found in the recent review by Liu et al. [5], and a series of challenging radiative transfer problems in combustion are described by Howell and Mengüç [6].

In this study, we focus on three main categories of RTE solvers, including the Monte Carlo method (MC), the spherical harmonics method, and the discrete ordinates method (DOM), and the performance of the full spectrum correlated k-distribution (FSK) spectral model. The two MC-based stochastic methods tested are the traditional Photon Monte Carlo (PMC) method and the quasi-Monte Carlo (QMC) method. The PMC is so far the most effective method, first formulated by Fleck [7], and Howell and Perlmutter [8]. Modest [9] improved the PMC to treat spectral properties. The QMC method is a modified version of the MC method which uses low-discrepancy sequences instead of random numbers [10]. The spherical harmonics method is a spectral method that approximates the angular distribution by a truncated series of spherical harmonics series [11–13]. Both the P_N method and the simplified P_N (SP_N) method with different orders are demonstrated in this study. The DOM discretizes the entire solid angle into discrete directions with assigned quadrature weights [14]. The accuracy and computational cost increase with the total number of discrete ordinates. The performances of selected numbers of discrete polar and azimuthal ordinates are benchmarked. Lastly, the FSK is a spectral model based on reordering the oscillatory absorption coefficients across the entire spectrum into corresponding k-distributions. The FSK is exact for homogeneous media, and the assumption of a correlated absorption coefficient is made for the nonhomogeneous media [15]. Employing the FSK reduces the number of evaluations of RTE from 1 million times to as low as eight times with high accuracy for regular combustion conditions.

The radiation models (i.e., RTE solvers and spectral models) are applied to evaluate the nongray radiative transfer in a turbulent piloted methane/air jet flame. The trade-offs between the accuracy, the computational cost, and the implementation difficulty are discussed in detail. All the deterministic solvers employed in this study are implemented using OpenFOAM programming framework [16] through its data structures and linear PDE solvers, while all the stochastic solvers and the spectral models used in this study are from an in-house Fortran library. The implementation details of the specific models can be found as follows: DOM [17], P_N [18], SP_N [19], PMC [20], QMC [10], LBL [21], and FSK [22]. All the solvers support distributed memory parallelism through MPI, but only the serial runs on a single core are benchmarked in this study.

RADIATION MODELS

The quasi-steady spectral radiative transfer equation (RTE) [20] is an integro-differential equation in five dimensions: three spatial coordinates and two directional coordinates, given by Eq. (1):

$$\frac{\mathrm{d}I_\eta}{\mathrm{d}s} = \kappa_\eta I_{b\eta} - \kappa_\eta I_\eta - \sigma_\eta I_\eta + \frac{\sigma_\eta}{4\pi}\int_{4\pi} I_\eta \Phi_\eta(\hat{\mathbf{s}}_i, \hat{\mathbf{s}}) d\Omega_i. \quad (1)$$

The dependent variable in this equation is radiative intensity $I_\eta(\mathbf{r}, \hat{\mathbf{s}})$. Here the subscript η denotes the spectral nature of the equation. $I_{b\eta}$ is the blackbody radiative intensity; κ_η is the absorption coefficient of the medium; σ_s is the scattering coefficient; $\Phi(\hat{\mathbf{s}}_i, \hat{\mathbf{s}})$ is the scattering phase function between ray directions $\hat{\mathbf{s}}_i$ and $\hat{\mathbf{s}}$; Ω_i represents the solid angle. In most combustion problems radiation enters as a source term (aka divergence of radiative heat flux or $\nabla \cdot \mathbf{q}$) in the energy equation which can be evaluated once the radiative intensity is known. Approximation for the angular distribution of the radiative intensity is required to solve the RTE for deterministic methods.

Discrete Ordinates Method

In the discrete ordinates method, the RTE, Eq. (1), is transformed into a system of first-order PDEs. This is accomplished by discretizing the directional variable $\hat{\mathbf{s}}$ into a set of N directions $\hat{\mathbf{s}}_i$ where $i = 1, 2, \ldots, N$, called ordinates. Each of these ordinates has a corresponding quadrature weight w_i. Solving the system of PDEs yields a set of partial intensities $I_{\eta,i}$ which, combined with the quadrature weights, can be used to approximate the radiative intensity via numerical quadrature.

The order of accuracy of the DOM depends on the number of ordinates N and corresponding quadrature weights. This directly determines the number of PDEs that must be solved. Therefore, with an increasing order, it is expected that the computational cost would also increase. In this paper, the ordinates are discretized uniformly along the polar and azimuthal angles. For example, for the case of $N = 2 \times 4$, two quadrature points are chosen in the polar direction and four quadrature points are chosen in the azimuthal direction, yielding a total of 2×4 ordinates.

Spherical Harmonics Method

The spherical harmonics method transforms the RTE into a set of simultaneous first-order or second-order PDEs. The general formulation of the method is to replace I_η by a truncated series of spherical harmonics of order N. This is given by

$$I_\eta(\mathbf{r}, \hat{\mathbf{s}}) = \sum_{n=0}^{N} \sum_{m=-n}^{n} I_{n,\eta}^{m}(\mathbf{r}) Y_n^m(\hat{\mathbf{s}}), \tag{2}$$

where $I_{n,\eta}^{m}(\mathbf{r})$ are the intensity coefficients which are functions of space only, and $Y_n^m(\hat{\mathbf{s}})$ are the spherical harmonics satisfying Laplace's equation in spherical coordinates. We use an axisymmetric formulation of P_N method and the corresponding Marshak's boundary condition [18] here with $(N+1)^2/4$ second-order elliptic PDEs.

The lowest order approximation of the P_N approximation, which is the P_1 method, is very popular and can be found in most commercial and academic software for radiative transfer. On the contrary, the high-order P_N method is rarely used in practice because of its cumbersome mathematics and implementation. The other option is the simplified P_N (SP_N) method [19, 23]. The SP_N method approximates the one-dimensional P_N formulation for a slab to a full three-dimensional configuration, which was originally proposed by Gelbard [24].

Monte Carlo Method

In the Monte Carlo method, a large number of photon bundles or rays are traced from their point of emission till their depletion or exit from the computational domain. This has led to the name photon Monte Carlo (PMC) method. Each photon bundle or ray is defined by its location, wavenumber, and direction of propagation. The total energy of the photon bundles emitted from a location is equal to the radiative emission from that location. As these bundles or rays travel through participating media, the media absorbs energy from the rays based on the wavenumber of the ray and the local spectral absorption coefficient. The net radiative heat flux is calculated by tracking the energy exchange between rays and the local media. The emission location, wavenumber, and direction of propagation for each ray are determined by sampling six independent random numbers – three for emission location (R_x, R_y, R_z), two for propagation direction (R_θ, R_ϕ), and one for wavenumber (R_η). The details of the random number relations can be found in [20].

Recently several researchers have proposed a quasi-Monte Carlo (QMC) method as a computationally efficient alternative for PMC [10, 25]. In QMC, the six random numbers are replaced by suitably chosen numbers from low-discrepancy sequences [26, 27]. This leads to a considerably lower statistical error even with a lower number of rays than conventional PMC. In this work, we use the Sobol sequence [28]. The details of the method and validation cases can be found in [10].

The PMC method is the most robust and most accurate method for RTE solver. In this work, the solution from PMC is treated as the benchmark reference solution.

Spectral Models

While the RTE solvers deal with the solution of the spectral RTE, spectral models deal with the evaluation of spectral properties (e.g., κ_η, σ_η, Φ_η). In this work we mainly use two spectral models - line-by-line (LBL) [2–4] and full spectrum k-distribution (FSK) [15, 22, 29] method. The LBL method, which is the most accurate spectral model, captures the spectral variation at the level of spectral lines. In the relevant range of wavenumbers, there are more than a million spectral lines required for appropriate accuracy. This means one would need to solve the RTE more than a million times (once for each line). This makes the use of LBL with a deterministic RTE solver such as DOM or P_N impractical. Stochastic Monte Carlo-based methods do not suffer from this limitation. Hence in this work we use LBL mostly with PMC and QMC. The details of the LBL database used can be found in [21].

The second spectral model used in this work is a full spectrum k-distribution lookup table [22] created using the full-spectrum correlated k-distribution (FSK) method [15, 29]. In FSK, the spectral properties are mapped from wavenumber space to g-space, which can be resolved by numerical quadrature. Therefore the complete evaluation of radiation requires only the solution of RTE at a small number of quadrature points. Several versions of lookup tables have been developed [22, 30, 31] – referred to as FSKTable. In this work we use the version in [22]. The FSKTable is used with DOM and P_N solvers in this work.

To establish a point of reference for different spectral mod-

els, we have also run a series of simulations with the P_1 solver, using a Planck-mean based gray approximation and the LBL database.

RESULTS

Target flame

Sandia Flame D is a turbulent piloted jet flame [32] with a Reynolds number of Re_D=22,400. The fuel from the main jet is a mixture of methane and air with a ratio of 1:3 by volume. The main jet with a diameter of $d_j = 7.2$ mm at the center is surrounded by an annular pilot with a diameter of $2.62d_j$ to stabilize the main jet. The pilot is a lean mixture of C_2H_2, H_2, air, CO_2 and N_2 with the fuel-air equivalence ratio ϕ being 0.77. The precise and careful measurement of Sandia Flame D provides a series of high quality experimental data [32] that makes it a standard benchmark of a turbulent jet flame to validate combustion models.

The effects of radiative transfer for the simulation of Sandia Flame D have been studied by Li [33], Wang [34], and Pal [35]. The importance of radiation and its interaction with turbulence (TRI) has been established by comparing the simulation results and the experimental measurements. Pal [35] also found that different spectral models and RTE solvers yield similar results because of the relatively small size of Sandia Flame D (though the small differences in predicted temperature resulted in large differences in predictions of NO). Since the size of turbulent jet flames in real applications tends to be much larger, Sandia Flame D was scaled four times (Sandia Flame D×4) to study the effects of radiation for optically thicker turbulent jet flames [33–35]. Sandia Flame D is scaled up in such a way that the diameter of the main jet and the outer diameter of the pilot are quadrupled while decreasing the exit velocity of the mixture out of the jet and pilot to keep the Reynolds number Re_D unchanged. The geometric sizes of the main jet and the pilot and the inlet velocities of the original Sandia Flame D and Sandia Flame D×4 are shown in Table 1. The co-flow represents the environmental air entering the wind tunnel.

TABLE 1. SIZES AND THE INLET VELOCITIES OF THE MAIN JET, THE PILOT, AND THE CO-FLOW [36]

	Sandia Flame D		Sandia Flame D×4	
	d (mm)	u (m/s)	d (mm)	u (m/s)
main jet	7.2	49.89	28.8	12.4725
pilot	18.864	10.57	75.456	2.6425
co-flow	258.2	0.90	1032.8	0.2250

Comparison of accuracy and cost

Different RTE solvers and spectral models are compared for a frozen-field snapshot of the quasi-stationary Sandia D×4 flame. The frozen-field snapshot is obtained on an axisymmetric mesh with 3325 finite volume cells with 35 cells along the radial direction, and 95 cells along the axial direction. The full size of the computational domain is 0.516 m × 2.88 m, and the mesh is refined to have a high-resolution region close to the jet. The contours of relevant scalars of the snapshot are shown in Fig. 1. The negative radiative heat source ($\nabla \cdot \mathbf{q}$) is computed on the finite volume mesh and sampled along three lines ($z/d = 14.93, 29.79, 44.65$ as marked in Fig. 1). The distribution of temperature and Planck-mean absorption coefficients along two of these lines are shown in Fig. 2 for reference. For the discrete ordinate method, 2×4, 4×4, 4×8, 4×16, 8×8, 8×16, and 16×32 ordinates are used. For the spherical harmonics (P_N) method, P_1, P_3, P_5, and P_7 are used as well as the simplified SP_3 and SP_5. For QMC, 100,000 rays are used, and for PMC, 1,000,000 rays are used. For PMC results, the standard deviation are plotted as error bars. In all cases, the PMC and QMC RTEs are used with a line-by-line (LBL) spectral model and DOM and P_N / SP_N solvers are coupled to the FSKTable using an eight-quadrature scheme. The open boundaries are treated as cold and black. Each combination of RTE and spectral model is benchmarked on a single Intel Xeon E5-2687W V4 CPU (3.00 GHz). All the comparisons in this work are based on the divergence of radiative heat flux ($\nabla \cdot \mathbf{q}$) or the negative radiative heat source term; and the PMC–LBL results are treated as benchmark reference.

To evaluate the accuracy of the FSKTable, first we present a comparison of FSKTable with LBL using the same RTE solver. In this case, we use the P_1 solver. The representative results along two lines ($z/d = 14.93, 44.65$) are shown in Fig. 3. We also show the results from P_1–Gray and Optically Thin models in this figure for references. Clearly, both the Optically Thin and the gray approximations lead to gross overestimation of $\nabla \cdot \mathbf{q}$. The results from FSK and LBL using the same RTE solver (P_1) match very well. This establishes the accuracy of the FSKTable in the current configuration and the validity of the correlated-k assumption. Hence, in subsequent comparisons, the differences in accuracy can be assumed to be stemming from the inaccuracy of the RTE solver and not due to inaccuracy of the spectral model.

The profile of $\nabla \cdot \mathbf{q}$ along the three lines for DOM and P_N/SP_N solvers are presented in Figs. 4 and 5, respectively. Their computational costs are shown in Table 2. Results from QMC are compared with PMC in Fig. 6 with their computational costs shown in Table 3. The DOM results show a reasonably accurate result at all axial locations lying within the error bars of the PMC. Interestingly, the higher orders DOM leads to slight overprediction than the lower orders due to the axisymmetric mesh and rotational invariant formulation as was previously reported [17]. In general, the error from DOM seems to be larger near the axis of

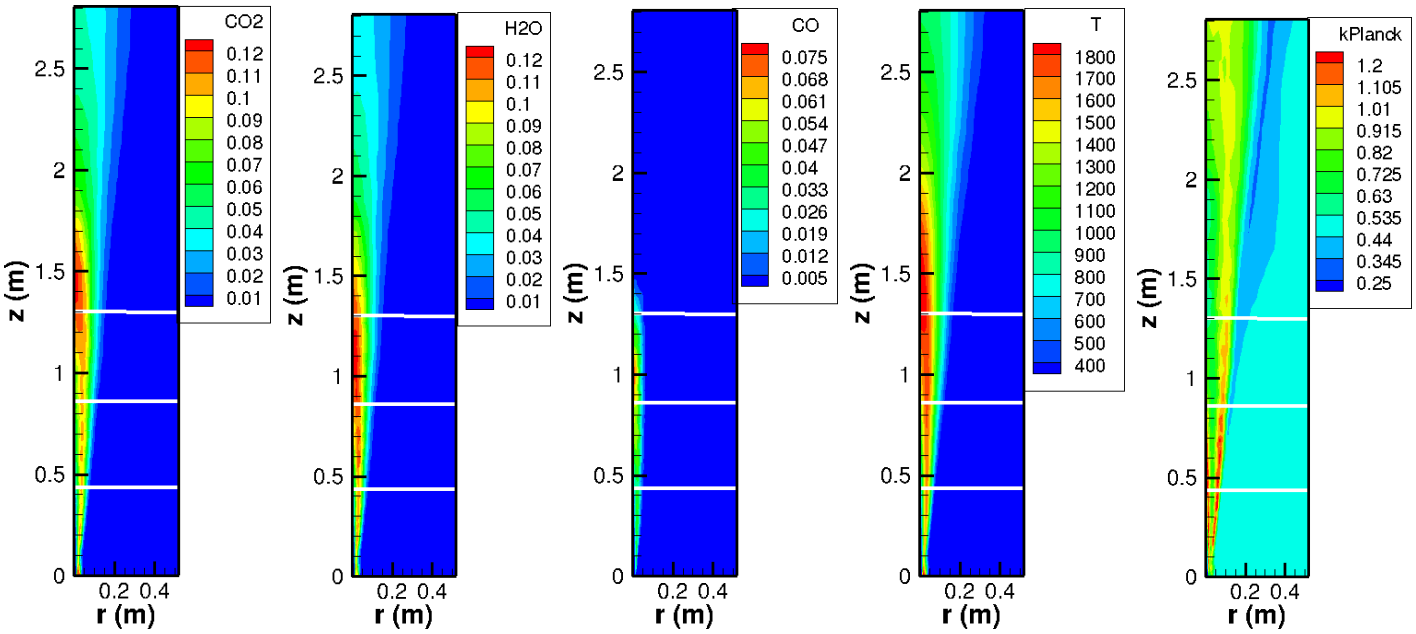

FIGURE 1. **CONTOUR PLOT OF THE SCALAR FIELDS FOR THE SNAPSHOT OF THE SANDIA D×4 FLAME.**

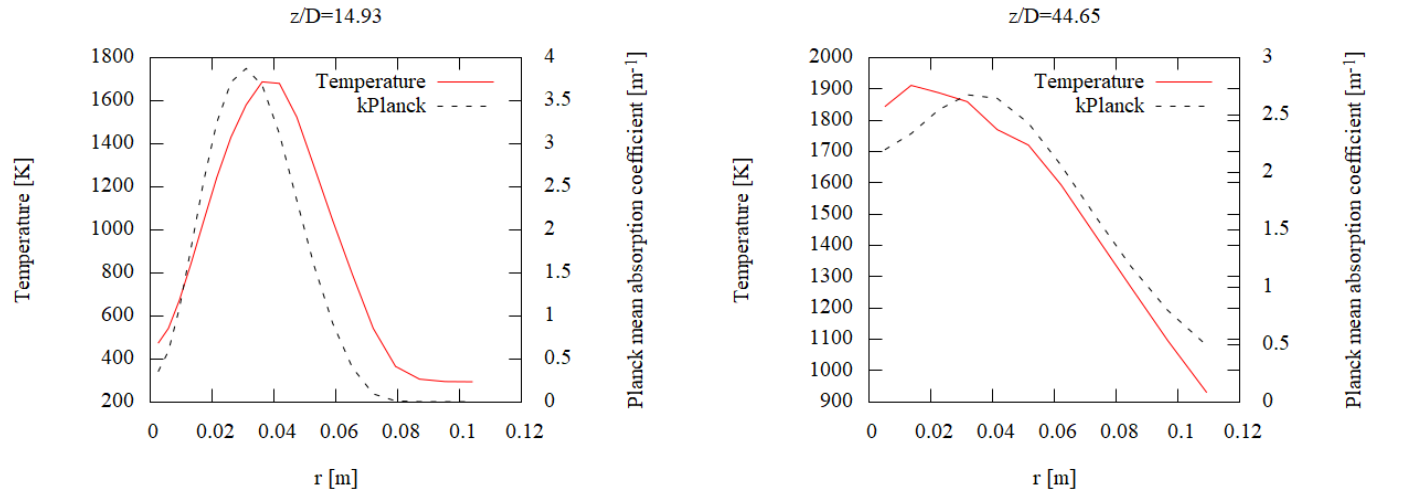

FIGURE 2. **TEMPERATURE AND PLANCK-MEAN ABSORPTION COEFFICIENT FOR FROZEN FIELD OF SANDIA D×4 FLAME AT TWO AXIAL LOCATIONS.**

the flame. The computational cost for DOM–FSK increases with the number of ordinates as expected.

As expected, for the P_N method, increasing the order of accuracy achieved results closer to PMC–LBL. However, the advantage of accuracy gained seems to get lower with the increase in order (i.e., the accuracy gained from moving to P_7 and P_5 from P_3 is less than that by moving to P_3 from P_1). Furthermore, P_1 performs rather poorly at all three axial locations. Both SP_3 and SP_5 perform well. Except for the $z/d = 44.65$ location, the SP_N solvers yield a solution within the error bars of the PMC-LBL results. It might be due to certain level of compensation of errors. Computational cost of P_N increased with increasing order of accuracy nonlinearly. The QMC results are almost always within the error bars of the PMC–LBL at an order of magnitude lower cost than PMC (see Fig. 6 and Table 3). This is similar to the results obtained in [10].

Finally, we present a comparison of DOM 4×4 and P_3 in Figure 7 for two representative lines at z/d =14.93 and 44.65.

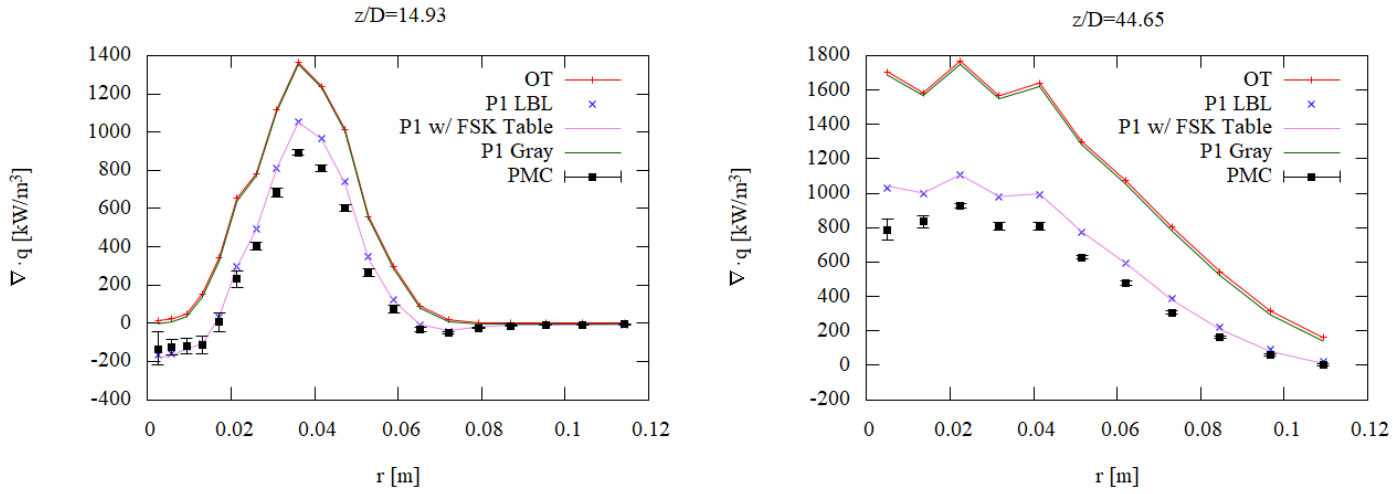

FIGURE 3. COMPARISON OF THE DIVERGENCE OF RADIATIVE HEAT FLUX ($\nabla \cdot \mathbf{q}$) FROM DIFFERENT SPECTRAL MODELS WITH THE P_1 SOLVER AT TWO AXIAL LOCATIONS.

TABLE 2. CPU TIMES FOR P_N AND DOM SOLVERS WITH FSK SPECTRAL MODEL

P_N and SP_N	CPU Time (s)	DOM	CPU Time (s)
P_1	1.66	DOM 2×4	1.75
P_3	2.60	DOM 4×4	2.47
P_5	5.05	DOM 4×8	3.45
P_7	10.47	DOM 4×16	6.84
SP_3	1.98	DOM 8×8	6.05
SP_5	3.49	DOM 8×16	12.54
		DOM 16×32	60.95

TABLE 3. CPU TIMES FOR PMC/QMC SOLVERS WITH LBL SPECTRAL MODEL

RTE	PMC	QMC
CPU Times (s)	33.84	4.32

We chose these two solvers for direct comparison as their computational costs are similar in this study. The comparison shows that P_3 overpredicts the divergence of heat flux whereas DOM almost always produces results within the error bar of the PMC.

The DOM results show the same trends as P_N results (see Fig. 4). If the number of ordinates used increases, the results more closely match PMC LBL accuracy. In general, most of the DOM results fall within the standard error of the PMC LBL results except for 2×4 and 4×4 ordinates. Similarly to the P_N results, the computational cost also increases significantly with an increased number of ordinates (see Table 2). In fact, the computational cost is directly proportional to the total number of ordinates. For example, in the case of 4×8 ordinates, there are half as many ordinates as the case of 4×16 and approximately half of the computational cost. Since the DOM results fall within PMC–LBL standard error if enough ordinates are used (at minimum 4×8), it may not be worth the extra computational cost to use a higher number of ordinates given the significant increase in computational cost.

In general, the QMC results achieve PMC LBL accuracy and at a fraction of the computational cost of the PMC runs. This is due to the fact that QMC shows a faster rate of decrease in statistical error with the increase in sample size seen than in PMC [10].

DISCUSSION

The target flame considered in this work is an artificial flame based on a laboratory-scale turbulent jet flame. While the comparisons of computational cost and accuracy shown here are specific to a large, nonsooting jet flame similar to the target flame, the results provide some insights into applicability of various radiation models in different configurations. The jet flame provides a significantly non-homogeneous distribution of participating media, leading to locally optically thick regions within rather optically thin medium (Fig. 1). This type of nonhomogenous distribution of absorption coefficient is characteristic of most turbulent combustion devices. One of the reasons behind artificially scaling up the original laboratory flame, as discussed in [33–35], is to specifically study large combustion systems. Radiation is a volumetric phenomenon, and therefore, the importance of ra-

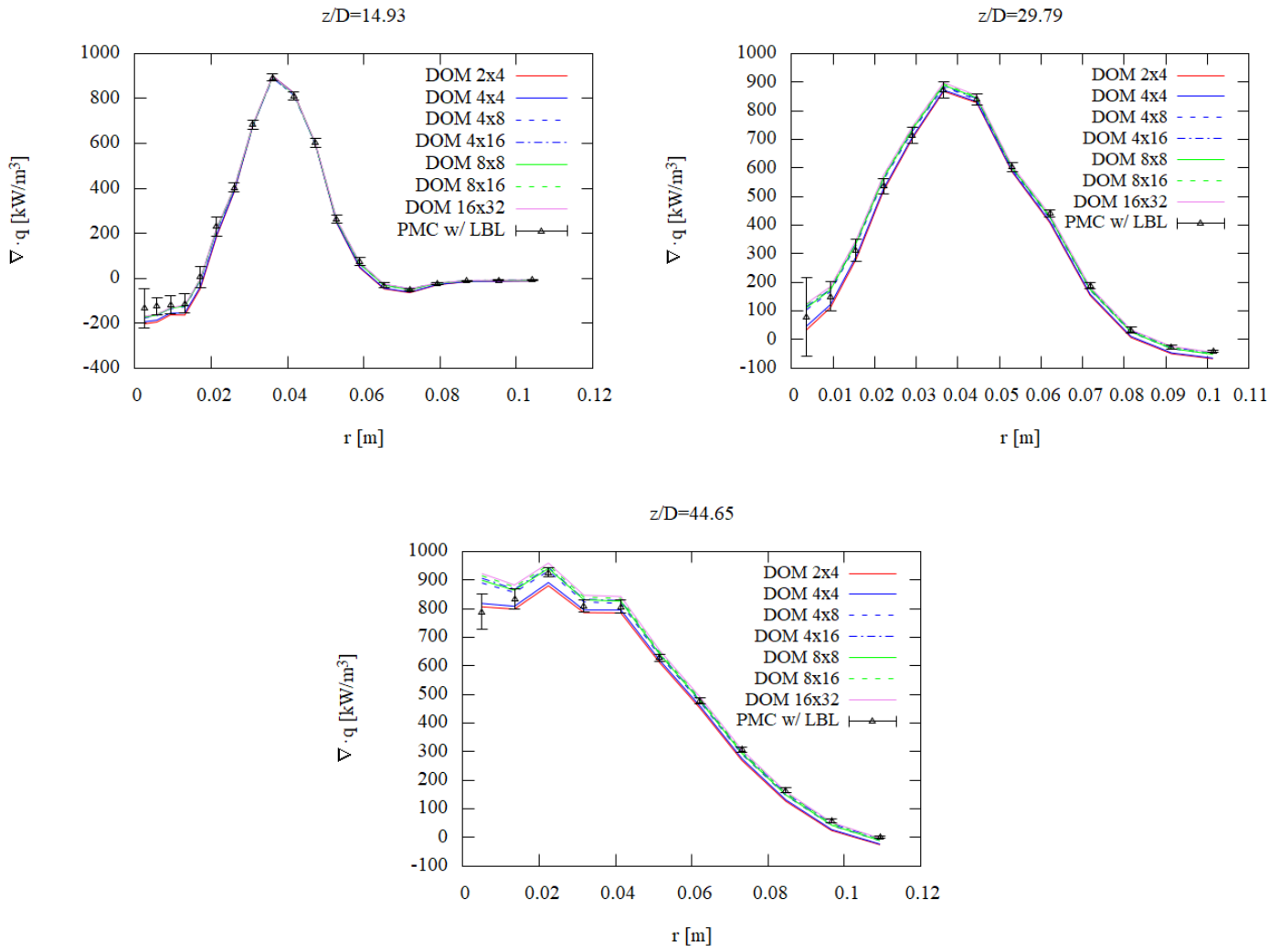

FIGURE 4. COMPARISON OF THE DIVERGENCE OF RADIATIVE HEAT FLUX ($\nabla \cdot \mathbf{q}$) FROM THE DOM–FSK METHODS AND THE PMC–LBL METHOD AT THREE AXIAL LOCATIONS.

diation is expected to be greater in large devices than in small laboratory-scaled flames. The size of the scaled flame is also somewhat representative of real combustion devices such as furnaces and gas turbines.

A second point of note is that the computational cost presented here includes the cost for evaluating both the spectral model and solving RTE. However, since all RTE solvers except PMC and QMC use FSKTable, the comparison of computational cost between P_N and DOM solvers will still be somewhat representative in any other configurations without scattering or reflecting walls as is the case for the current target. If scattering or reflecting walls are present in the configuration, the computational cost of PMC, QMC, and P_N is expected to be affected only marginally as their formulations or solution algorithms are not affected. But for the DOM, the resultant PDEs can be treated as a set of uncoupled PDEs if there are no scattering or reflecting walls leading to a lower cost in these scenarios. Furthermore, the computational cost of RTE solvers can be optimized on a case-by-case basis by tuning the number and order of iterations performed in the solver in the actual implementation of the RTE solver. Such optimizations have not been done in the current work. Hence, in this work we present Table 2 as a qualitative comparison of the relative cost of different RTE solvers.

CONCLUSION

In this work different orders of DOM and P_N solvers with an FSK spectral model are compared with the benchmark ref-

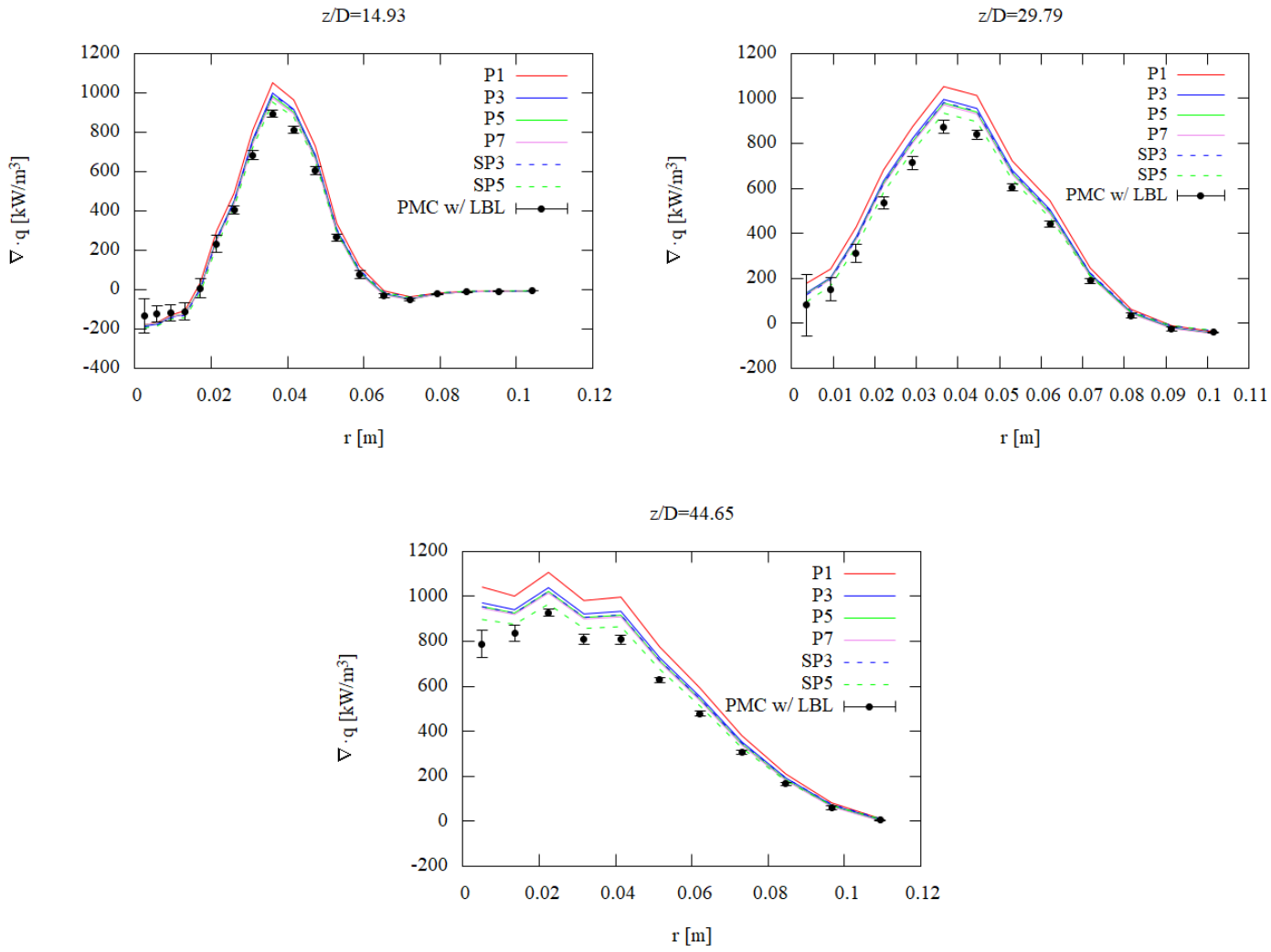

FIGURE 5. **COMPARISON OF THE DIVERGENCE OF RADIATIVE HEAT FLUX ($\nabla \cdot \mathbf{q}$) FROM DIFFERENT ORDERS OF THE P_N–FSK, SP_N–FSK METHODS AND THE PMC-LBL METHOD AT THREE AXIAL LOCATIONS.**

erence solution from PMC with LBL for a scaled turbulent jet flame. First, to illustrate the difference in results due to the spectral model, we show the radiative source terms ($\nabla \cdot \mathbf{q}$) calculated using P_1 with both LBL and FSK in Fig. 3. This comparison shows that the FSK lookup table provides a reliable estimation of spectral properties as the results of P_1-LBL and P_1-FSK overlap completely. Then, we present the results from a series of DOM and P_N solvers of different orders in Figs. 4 and 5. In the current configuration DOM provides a reasonably accurate estimate of the radiative source term even with low resolution such as 2×4 where the results almost always lie within the error bars of the PMC solution (except near the axis at $z/D = 44.65$ location). The solutions of the P_N solvers show a clear trend of increasing accuracy with the order. In general, P_1 performs rather poorly in this case. However, the simplified P_N versions – SP_3 and SP_5 – provide an accurate estimation of the radiative source term at a very low cost. Yet, since SP_N is a simple extrapolation of the one-dimensional configuration to three-dimensional configuration, this level of accuracy may not always be achievable for SP_N for all combustion configurations, particularly cases with complex geometry and strong nonhomogeneity. The comparison of P_3 with DOM 4×4 (Fig. 7) shows that in this case DOM performs better than spherical harmonics method at roughly the same computational cost. However, as discussed earlier, the relative computational cost of DOM and P_N may be affected if scattering or reflecting walls are included in the configuration. Additionally, we also show that the quasi-Monte Carlo method, an alternative to PMC, provides results as accurate as PMC using a

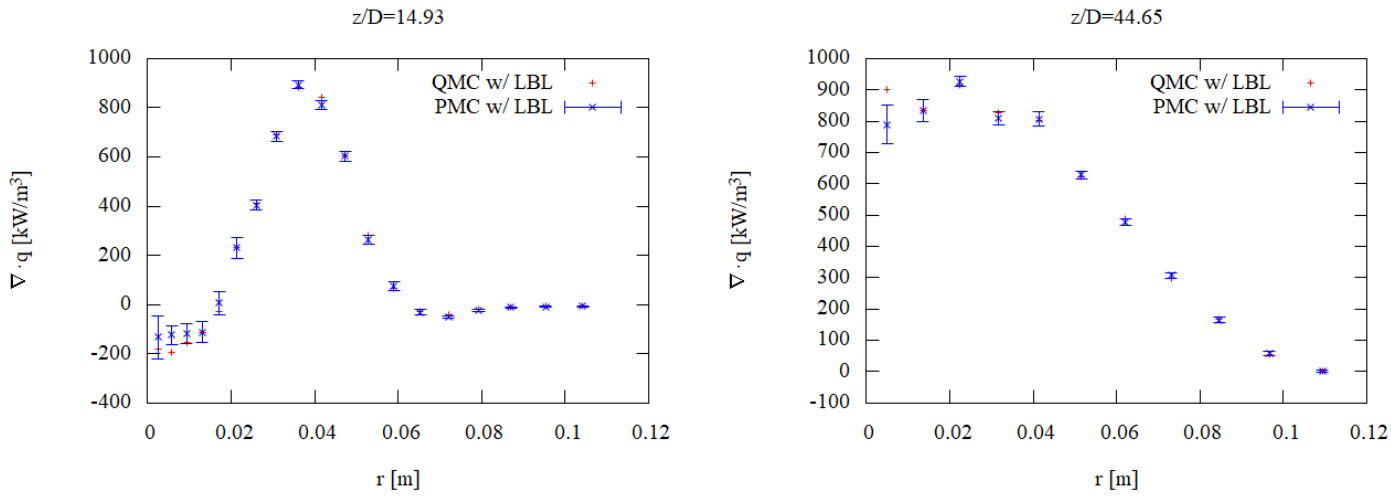

FIGURE 6. **COMPARISON OF THE DIVERGENCE OF RADIATIVE HEAT FLUX ($\nabla \cdot \mathbf{q}$) FROM PMC–LBL AND QMC–LBL METHODS.**

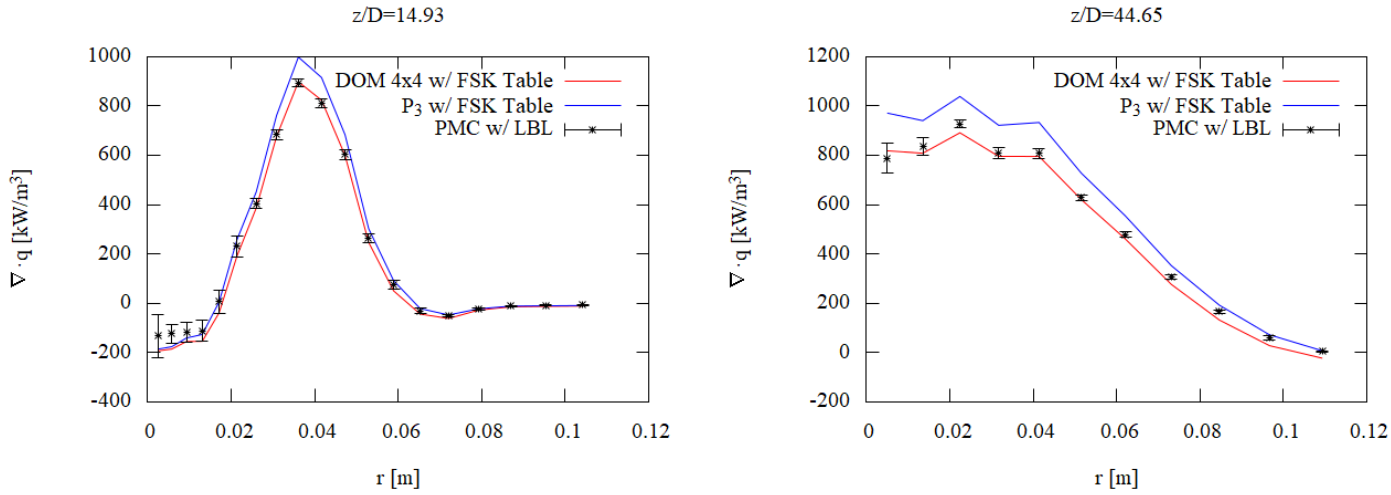

FIGURE 7. **COMPARISON OF THE DIVERGENCE OF RADIATIVE HEAT FLUX ($\nabla \cdot \mathbf{q}$) FROM P_3-FSK, DOM 4×4-FSK AND PMC-LBL METHODS.**

smaller number of rays.

ACKNOWLEDGEMENT

This research was supported by National Science Foundation and the Department of Energy through Grant No. NSF1258635 (WG, MFM, SR), and by the National Science Foundation under Grant No. 1756005 (CD, SR). WG and RS acknowledge the support from the Exascale Computing Project (17-SC-20-SC), a collaborative effort of the U.S. Department of Energy Office of Science and the National Nuclear Security Administration.

REFERENCES

[1] Modest, M. F. and Haworth, D. C., 2016, *Radiative Heat Transfer in Turbulent Combustion Systems*, Springer Verlag, New York.

[2] Gordon, I. E., Rothman, L. S., Hill, C., Kochanov, R. V., Tan, Y., Bernath, P. F., Birk, M., Boudon, V., Campargue, A., Chance, K. V., Drouin, B. J., Flaud, J. M., Gamache, R. R., Hodges, J. T., Jacquemart, D., Perevalov, V. I., Perrin, A., Shine, K.P., Smith, M. A. H., Tennyson, J., Toon, G. C., Tran, H., Tyuterev, V. G., Barbe, A., Császár, A. G., Devi, V. M., Furtenbacher, T., Harrison, J. J., Hartmann, J. M., Jolly, A., Johnson, J., T, Karman, T., Kleiner, I., Kyuberis,

A. A., Loos, J., Lyulin, O. M., Massie, S. T., Mikhailenko, S. N., Moazzen-Ahmadi, N., Müller, H. S. P., Naumenko, O. V., Nikitin, A. V., Polyansky, O. L., Rey, M., Rotger, M., Sharpe, K., S. W.and Sung, Starikova, E., Tashkun, S. A., Vander Auwera, J., Wagner, G., Wilzewski, J, Wcisło, P., Yu, S., and Zak, E.J., 2017, "The HITRAN2016 molecular spectroscopic database", *Journal of Quantitative Spectroscopy and Radiative Transfer*, **203**, pp. 3–69.

[3] Rothman, L. S., Gordon, I. E., Barber, R. J., Dothe, H., Gamache, R. R., Goldman, A., Perevalov, V. I., Tashkun, S. A., and Tennyson, J., 2010, "HITEMP, the high-temperature molecular spectroscopic database", *Journal of Quantitative Spectroscopy and Radiative Transfer*, **111**(15), pp. 2139–2150.

[4] Tashkun, S. A. and Perevalov, V. I., 2011, "CDSD-4000: High-resolution, high-temperature carbon dioxide spectroscopic databank", *Journal of Quantitative Spectroscopy and Radiative Transfer*, **112**(9), pp. 1403–1410, available from ftp://ftp.iao.ru/pub/CDSD-4000.

[5] Liu, F., Consalvi, J. L., Coelho, P. J., André, F., Gu, M., Solovjov, V., and Webb, B., 2020, "The impact of radiative heat transfer in combustion processes and its modeling–with a focus on turbulent flames", *Fuel*, **281**, p. 118555.

[6] Howell, J. R. and Mengüç, M. P., 2018, "Challenges for radiative transfer 1: towards the effective solution of conjugate heat transfer problems", *Journal of Quantitative Spectroscopy and Radiative Transfer*, **221**, pp. 253–259.

[7] Fleck, J. A., 1961, "The calculation of nonlinear radiation transport by a Monte Carlo method", Technical Report UCRL-7838, Lawrence Radiation Laboratory.

[8] Howell, J. R. and Perlmutter, M., 1964, "Monte Carlo solution of radiant heat transfer in a nongrey nonisothermal gas with temperature dependent properties", *AIChE Journal*, **10**(4), pp. 562–567.

[9] Modest, M. F., 1992, "The Monte Carlo method applied to gases with spectral line structure", *Numerical Heat Transfer, Part B Fundamentals*, **22**(3), pp. 273–284.

[10] Farmer, J. and Roy, S., 2020, "A quasi-Monte Carlo solver for thermal radiation in participating media", *Journal of Quantitative Spectroscopy and Radiative Transfer*, **242**, p. 106753.

[11] Modest, M. F. and Yang, J., 2008, "Elliptic PDE formulation and boundary conditions of the spherical harmonics method of arbitrary order for general three-dimensional geometries", *Journal of Quantitative Spectroscopy and Radiative Transfer*, **109**, pp. 1641–1666.

[12] McClarren, R. G., Evans, T. M., Lowrie, R. B., and Densmore, J. D., 2008, "Semi-implicit time integration for PN thermal radiative transfer", *Journal of Computational Physics*, **227**(16), pp. 7561–7586.

[13] Ge, W., Modest, M. F., and Roy, S. P., 2016, "Development of high-order PN models for radiative heat transfer in special geometries and boundary conditions", *Journal of Quantitative Spectroscopy and Radiative Transfer*, **172**, pp. 98–109.

[14] Coelho, P. J., 2014, "Advances in the discrete ordinates and finite volume methods for the solution of radiative heat transfer problems in participating media", *Journal of Quantitative Spectroscopy and Radiative Transfer*, **145**, pp. 121–146.

[15] Modest, M. F. and Zhang, H., 2002, "The full-spectrum correlated-*k* distribution for thermal radiation from molecular gas–particulate mixtures", *ASME Journal of Heat Transfer*, **124**(1), pp. 30–38.

[16] Jasak, H., Jemcov, A., and Tukovic, Z., 2007, "OpenFOAM: A C++ library for complex physics simulations", In *International Workshop on Coupled Methods in Numerical Dynamics*, Dubrovnik, Croatia, IUC, pp. 1–20.

[17] Cai, J., Roy, S., and Modest, M. F., 2016, "A comparison of specularly reflective boundary conditions and rotationally invariant formulations for discrete ordinate methods in axisymmetric geometries", *Journal of Quantitative Spectroscopy and Radiative Transfer*, **182**, pp. 75–86.

[18] Ge, W., Modest, M. F., and Marquez, R., 2015, "Two-dimensional axisymmetric formulation of high order spherical harmonics methods for radiative heat transfer", *Journal of Quantitative Spectroscopy and Radiative Transfer*, **156**, pp. 58–66.

[19] Modest, M. F., Cai, J., Ge, W., and Lee, E., 2014, "Elliptic formulation of the simplified spherical harmonics method in radiative heat transfer", *International Journal of Heat and Mass Transfer*, **76**, pp. 459–466.

[20] Modest, M. F., 2013, *Radiative Heat Transfer*, Academic Press, New York, 3rd ed.

[21] Ren, T. and Modest, M. F., 2019, "Line-by-line random-number database for Monte Carlo simulations of radiation in combustion system", *ASME Journal of Heat Transfer*, **141**.

[22] Wang, C., Ge, W., Modest, M. F., and Cai, J., 2016, "A full-spectrum *k*-distribution look-up table for radiative transfer in nonhomogeneous gaseous media", *Journal of Quantitative Spectroscopy and Radiative Transfer*, **168**, pp. 45–56.

[23] Hamilton, S. P. and Evans, T. M., 2015, "Efficient solution of the simplified PN equations", *Journal of Computational Physics*, **284**, pp. 155–170.

[24] Gelbard, E. M., 1960, "Application of spherical harmonics method to reactor problems", *Bettis Atomic Power Laboratory, West Mifflin, PA, Technical Report No. WAPD-BT-20*.

[25] Palluotto, L., Dumont, N., Rodrigues, P., Gicquel, O., and Vicquelin, R., 2019, "Assessment of randomized Quasi-Monte Carlo method efficiency in radiative heat transfer simulations", *Journal of Quantitative Spectroscopy and Radiative Transfer*, **236**, p. 106570.

[26] Niederreiter, H., 1988, "Low-discrepancy and low-

dispersion sequences", *Journal of Number Theory*, **30**, pp. 51–70.

[27] Niederreiter, H., 1992, *Random number generation and Quasi-Monte Carlo methods*, Society for Industrial and Applied Mathematics.

[28] Sobol, I. M., 1976, "Uniformly distributed sequences with an additional uniform property", *USSR Computational Mathematics and Mathematical Physics*, **16**, pp. 236–242.

[29] Cai, J. and Modest, M. F., 2013, "Improved full-spectrum *k*-distribution implementation for inhomogeneous media using a narrow-band database", *Journal of Quantitative Spectroscopy and Radiative Transfer*, **141**, pp. 65–72.

[30] Wang, C., Modest, M. F., and He, B., 2016, "Full-spectrum *k*-distribution look-up table for nonhomogeneous gas-soot mixtures", *Journal of Quantitative Spectroscopy and Radiative Transfer*, **176**, pp. 129–136.

[31] Zhou, Y., Wang, C., and Ren, T., 2020, "A machine learning based efficient and compact full-spectrum correlated *k*-distribution model", *Journal of Quantitative Spectroscopy and Radiative Transfer*, **254**, p. 107199.

[32] Barlow, R. S. and Frank, J. H., 1998, "Effects of turbulence on species mass fractions in methane/air jet flames", In *Twenty-seventh Symposium (International) on Combustion*, **27**, The Combustion Institute, pp. 1087–1095.

[33] Li, G. and Modest, M. F., 2002, "Application of composition PDF Methods in the investigation of turbulence–radiation interactions", *Journal of Quantitative Spectroscopy and Radiative Transfer*, **73**(2–5), pp. 461–472.

[34] Wang, A., 2007, *Investigation of turbulence–radiation interactions in turbulent flames using a hybrid FVM/particle-photon Monte Carlo approach*, PhD thesis, The Pennsylvania State University, University Park, PA.

[35] Pal, G., Gupta, A., Modest, M. F., and Haworth, D. C., 2015, "Comparison of accuracy and computational expense of radiation models in simulation of nonpremixed turbulent jet flames", *Combustion and Flame*, **162**(6).

[36] Pal, G., 2010, *Spectral modeling of radiation in combustion systems*, PhD thesis, The Pennsylvania State University, University Park, PA.